ISABE 99-7275

A RANS METHOD FOR THE TIME-ACCURATE SIMULATION OF WAKE-INDUCED BOUNDARY-LAYER TRANSITION IN TURBINE FLOWS

F. Eulitz

DLR - Institute of Propulsion Technology
Linder Höhe, 51147 Köln
Germany

Abstract

A time-accurate multistage Navier-Stokes solver has been extended to simulate wake-induced transition in unsteady multistage turbomachinery flow. To this end, the Spalart-Allmaras turbulence model has been modified in several ways and coupled to a transition correlation on the basis of new modeling approaches by other authors.

Application to an unsteady test case, a turbine cascade subject to the wake of a moving bar, shows very good agreement with the measurements. First, the turbine cascade is considered without any wake disturbance at two Reynolds numbers. It is shown that the model is capable of simulating laminar separation-bubble induced transition and reproducing correctly the observed Reynolds number effects. In the unsteady case, no separation occurs due to wake-induced transition. The migration of the transition start location is in remarkably good agreement with hot film measurement data.

Nomenclature

E	hot film anemometer output voltage
E_0	E at zero flow
f	frequency
H	boundary-layer shape factor, δ^*/θ
k	turbulent kinetic energy
L	blade length
p	pressure
t	time variable
T	wake passing period
Tu	freestream turbulence intensity
y^+	law-of-the-wall coordinate
Re_θ	Reynolds number, $u_E \theta / \nu_E$
Sr	Strouhal number

Greek Symbols

δ^*	displacement thickness
θ	momentum loss thickness
ν	kinematic viscosity
ν_T	eddy viscosity
τ_w	wall shear stress

Subscripts

0	stagnation flow
w	wall
RMS	root mean square

Abbreviations

S	separation start
T	transition start
R	reattachment

Introduction

The boundary-layer state determines to a large extent the performance, the loss production, and heat transfer of turbomachinery components. Especially at low Reynolds number operation, prolonged regions of laminar or transitional boundary-layers may exist. Very often, a further optimization of compressor and turbine components with respect to overall efficiency, fuel consumption, and manufacturing costs only seems possible when laminar-turbulent transition effects are taken into account. The need to better understand and manage its complex physics has led to an increasing number of experimental and theoretical investigations[1,16,21,29]. Widely, the different routes and causes for the boundary-layer to transition from laminar to turbulent flow have been classified into natural and by-pass transition, separated flow, and wake-induced transition[18,30]. According to Mayle[18], transition may be of 'multi-moded' nature, that is, different modes of the transition process may overlap in time and space. In particular, the

20000208 070

wakes of an upstream blade row represent a substantial source for the time-periodic disturbance of the boundary-layer which superimposes on the transition route the boundary-layer takes without interference with the wake.

While CFD, based on the numerical solution of the Reynolds averaged Navier-Stokes equations, is keeping on penetrating the aerodynamic design process, transition modeling is becoming a subject of increasing importance. Whereas wake-induced transition is not a point in steady-state calculations, it is a crucial ingredient for meaningful time-resolved studies of aerodynamic blade-row interaction. Understanding and exploiting the clocking effect[22], for example, represents an application of technical relevance for time-accurate CFD[5,6,10,11].

As transition modeling for unsteady turbomachinery flow is still in its infancy, transition effects are generally not accounted for in time resolved CFD applications. Halstead et al.[16] discuss results obtained with the unsteady boundary-layer code (using a $k - \varepsilon$ turbulence) by Fan & Lakshminarayana[14] and conclude that "no reliable means to compute these flows is yet available". For steady-state flows and simple configurations, however, some approaches, such as algebraic models based on the intermittency concept or low-Reynolds number turbulence models with or without additional modification[26,27] have been developed with varying degrees of success[24].

The goal of the paper is to present a Reynolds-averaged solution method which allows to include turbulence and transition effects for time-resolved multistage flow simulations. To this end, the Navier-Stokes solver TRACE-U, which has been developed over the last years at the DLR specifically for unsteady turbomachinery flow[7,11], is refined. The modeling approach taken here is defined, on the one hand, by the high computational costs of time-accurate multistage flow calculations and, on the other hand, the admission that a Reynolds-averaged eye is mostly blind of flow scales, which truly determine the transition physics. The consequence of the former is the use of parallel processing and that of the latter, a semi-empiric modeling methodology. For engineering use, accuracy and physical content are as important as numerical robustness and ease of handling.

The turbulence and transition model is based on the one-equation transport model by Spalart & Allmaras[25], which has been modified in several ways to incorporate freestream turbulence effects and to account for transition. Doing this, the new ideas by Mayle & Schulz[19] to calculate pretransitional boundary-layers and by Volino[28] to incorporate freestream turbulence effects were applied and adapted.

Numerical Method

The numerical method TRACE-U has been developed over the decade to accurately simulate unsteady turbomachinery flow on parallel distributed memory computers. It is being applied by a growing user community both in research and industry. As more detailed reports on the numerical method can be found in Engel et al.[7, 8] and Eulitz et al.[9,11,12], only a brief description is given here.

The two-dimensional or three-dimensional time dependent Reynolds-averaged Navier-Stokes equations are solved in a rotating frame of reference for the compressible ideal gas in conjunction with a turbulence model. The convective fluxes are discretized using Roe's TVD upwind scheme which is combined with van Leer's MUSCL extrapolation to obtain second order accuracy in space. For initialization, the flow solver is run in a steady-state multistage mode with an implicit time integration technique[12]. At the inlet and outlet boundaries of the computational domain, quasi-three dimensional non-reflecting boundary conditions according to Saxer and Giles are implemented. The bladerow interfaces are coupled through passage-averaged flow quantities and treated as entry or exit boundaries. For the unsteady calculation, a second-order time-accurate four-stage Runge-Kutta scheme is applied in combination with a time-consistent two-grid method to extent its numerical stability limit. Time accurate coupling of the moving and non-moving grid interface is realized by the sheared-cell technique. At the inlet and outlet boundaries, the non-reflecting method of Giles is employed.

To allow for an efficient and easy use of distributed memory computers, a subsystem was developed to handle the interprocessor communication and the control of the distributed program execution. As the parallel subsystem has been capsulated from the flow solver, no explicit parallelization work is necessary when adding new models or numerical methods to the code. Owing to the use of standard communication libraries (PVM or MPI), the code is hardware independent and currently run on a wide variety of distributed or shared memory computer systems.

Turbulence and Transition Modeling

Although Reynolds averaging and the Boussinesq assumption may strictly be inadequate concepts for the Navier-Stokes simulation of transitional and highly unsteady flow, it is in the light of its technical importance for modern turbomachinery design and the computational requirements of more rigorous approaches, worth going this semi-empiric route for engineering application.

Turbulence closure is based on the one-equation

transport model by Spalart & Allmaras[25] (SA). Formulated in terms of the eddy-viscosity and derived from physical reasoning, it has turned out to be a very competitive model when compared with more established Boussinesque models[3]. The SA model has been extended and adapted in various ways to allow for its application to unsteady and transitional flows with wake blade row interaction:

- The low-Reynolds formulation has been modified to yield proper asymptotic behavior of the viscous damping function when approaching the freestream edge of the boundary-layer.

- The destruction term has been modified for a better performance in flows with laminar separation-bubble induced transition.

- An additional production term has been introduced to incorporate freestream turbulence effects motivated by the new approach of Mayle & Schulz[19] to calculate the pretransitional fluctuations inside the boundary-layer and Volino's model[28] to include freestream turbulence effects.

- The original production term has been modified in order to allow for its gradual activation and deactivation similar to the approach by Schmidt & Patankar[20]. For the transition length, no explicit transition correlation is used. However, a transition correlation is used to detect the start of transition.

- The transition correlation by Drela[4] is used. It supplies the start of transition in term of the boundary-layer momentum thickness. The key parameters of the correlation are the boundary-layer shape parameter and the turbulence intensity.

Note that the task of modifying a one-equation model without compromising its original range of validity is much easier than attempting it with a two-equation transport model. As the SA-model, like any other Boussinesq-model, is completely void of transition physics, it needs in one or the other way to be informed about transition. This is done here by using a transition correlation and by modification of the production term. Details on the development of the turbulence and transition model and its validation can be found in a work by Eulitz[13].

Demonstration

In the course of its development, the numerical method has been compared against a large number of steady and unsteady test cases[7-12]. As agreement or disagreement with measurement data of complex flows may be coincidental, much effort has been spent in a

step-by-step validation of increasing flow complexity, e.g starting from unsteady linear theory[8] and ending up with 3D flows with shock/boundary-layer interaction and self-excited unsteadiness[13]. To assess the turbulence and transition modeling, in the following, a turbine cascade subject to the wake perturbation of an upstream moving bar is considered.
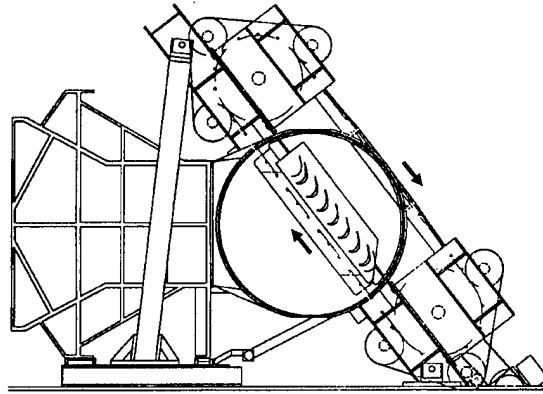

Figure 1. Setup of experiment: Turbine cascade with moving bar facility, from Acton & Fottner[1,2].

Description of Test Case

For the experimental investigation of unsteady wake-induced boundary-layer transition a wake generator was designed and built by Acton & Fottner[1,2] to be mounted on a high-speed cascade wind tunnel, figure 1. Special care had been taken to preserve the similarity parameters of turbine flow (e.g. wake width and velocity defect, turbulence intensity, and Strouhal number), table 1. As can be seen from the sketch in figure 1, cylindrical bars are mounted on a pair of rubber belts which are moving around the cascade. On their way forward, the bars generate the desired unsteady wakes, on their way backward, the bars are sufficiently downstream of the cascade to have negligible influence on the cascade flow. In the experiment, the configuration was examined for different values of the diameter d, speed u_{bar} and pitch P of the bars. Here, numerical results will be shown for d=2mm, u_{bar}=40 m/s and a pitch being the same as that of the blades (P=80mm). In table 1, the primary flow parameters with the Mach number at entry (1) and exit (2) of the cascade are shown. The given Reynolds number Re_{2th} of the flow is based on blade length and isentropic exit flow conditions. Re_d is the Reynolds number based on the bar diameter and the inflow conditions.

Ma_1	Ma_2	Re_{2th}	Re_d	Sr	Tu_1
0.21	0.4	$2 \cdot 10^5$	3150	0.8	1.8%

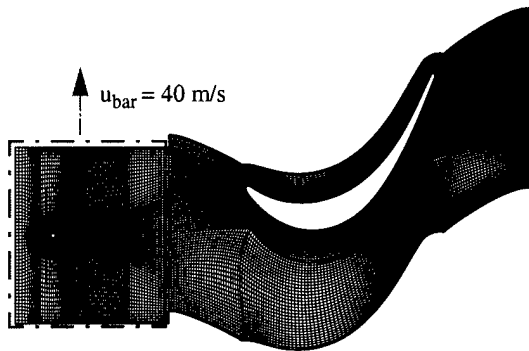Table 1: Primary flow parameter of unsteady test case.

Figure 2. Numerical model of moving-bar experiment using a multiblock computational mesh.

The two-dimensional numerical model of the experiment, which covers both the bar and the cascade, is shown in figure 2. In the multistage flow solver, the moving bar is logically treated as a rotor. Highly condensed O-mesh blocks with dimensions 61x41 for the bar and 291x35 for the blade have been used to adequately resolve the boundary-layer flow at the solid walls. The first node off the wall has been set within a distance of $y^+<1.5$ in inner wall coordinates. With 71 nodes in circumferential direction at the interface of the moving bar and the turbine meash blocks, the grid has been made rather fine in order to resolve the wake on its way through the turbine passage. In total, the mesh contains 29618 nodes.

Undisturbed Case: Reynolds number Effects

First, a steady-state calculation without any wake perturbation is performed in order to initialize the flow field. Further, to check if the current method is capable to reproduce Reynolds number effects in transitional flows with a laminar separation-bubble, another steady-state calculation with a higher Reynolds number, $Re_{2th}=3\cdot10^5$, has been performed. In figure 3, the measured and predicted pressure distributions are compared for the two Reynolds numbers. One can observe excellent agreement between the experimental and numerical data. It is known that the shape of the pressure distribution near the rearward suction side depends in a very sensitive way on the extent and location of the laminar separation-bubble and, thus, on the transition[17]. It is the region where the Reynolds number most effectively influences the pressure distribution. At lower Re_{2th}, the pressure gradient levels off in a more pronounced way before it recovers again in the transitional zone.

Shown in figure 4 are various boundary-layer parameters. As can be expected from the pressure distribution, the size of the laminar separation-bubble is larger at the lower Reynolds number. In laminar flow boundary-lay-

ers, a shape parameter H higher than 4 indicates separation profiles. For the laminar flat-plate boundary-layer (H=2.59), the skin friction scales with the inverse of the root of the Reynolds number, $c_f \sim 1/\sqrt{Re}$. This Reynolds number effect is well reproduced along the forward half (up to x/L=0.6) of the suction-side, where the shape parameter is very close to 2.6. Transition start can be detected from the steepening c_f-gradient in the reverse flow region. At the higher Reynolds number, transition occurs earlier and even upstream of the separation point; only a tiny separation-bubble forms.
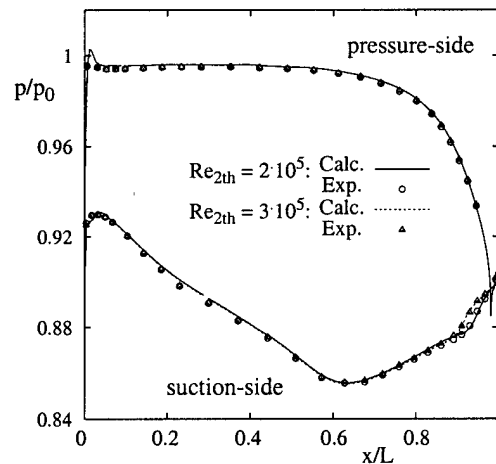

Figure 3. Comparison of measured and predicted surface pressure distribution at two Reynolds numbers.
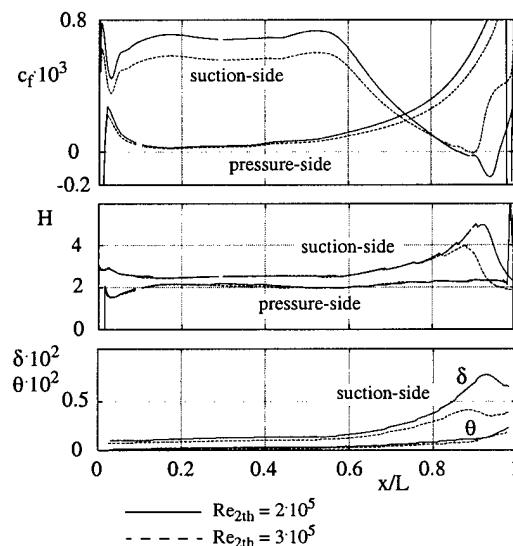

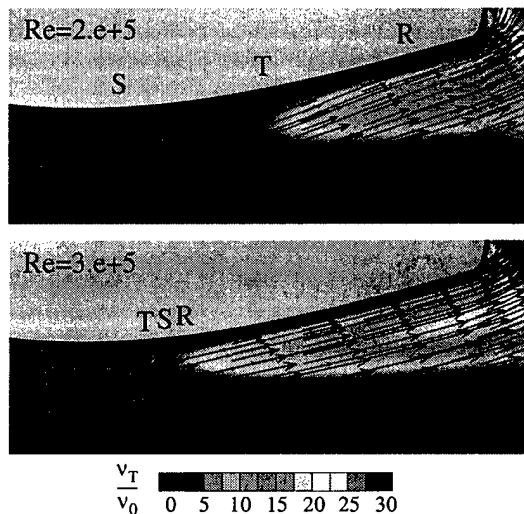Figure 4. Predicted boundary-layer parameters for the undisturbed cascade flow at two Reynolds numbers.

Figure 5. Streamlines, velocity vectors, and eddy-viscosity distribution for different Reynolds numbers.

The streamlines and velocity vectors shown in figure 5 give an impression of the Reynolds number effects. The background color shows where the turbulence model, triggered by the transition correlation, starts to produce eddy-viscosity.

Wake Disturbed Case

In the unsteady case, the bar is moving with a speed of 40 m/s giving rise to a wake passing frequency of 500 Hz and a a reduced frequency ($f \cdot L/c$) of 0.8.

Unsteady Flow Field

Figure 6 shows instantaneous distributions of the absolute density gradient and the eddy-viscosity. As expected from the Reynolds number of the cylinder $Re_d=3150$, a v.Karman vortex street forms in the wake of the moving bar. A FFT-analysis of an unsteady pressure signal of the moving wake reveals frequencies of higher amplitude in the range of 10 to 12.5 kHz (figure 7). This corresponds to an average Strouhal number ($f \cdot D/w$) of 0.215. Also, at the trailing edge of the turbine blade v.Karman vortices can be observed. Giving an impression similar to a Schlieren picture, the distribution of the density gradient (figure 6), shows that the v.Karman vortices induce pressure fluctuations which quickly spread into all directions. With rather low values of the momentum thickness (see figure 4), the boundary-layer of the *pressure-side* never satisfies the transition criterion, and thus remains entirely laminar. On the rearward *suction-side* of the profile, however, there is a transitional zone (the beginning of which is marked by an arrow in the eddy-viscosity plot of figure 6).
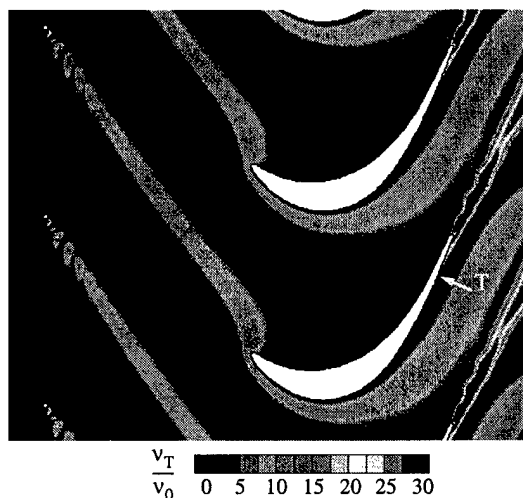

Figure 6. Instantaneous distributions at a chosen time instant, $t=t_0$: of the density gradient (top) and of the eddy-viscosity (bottom).
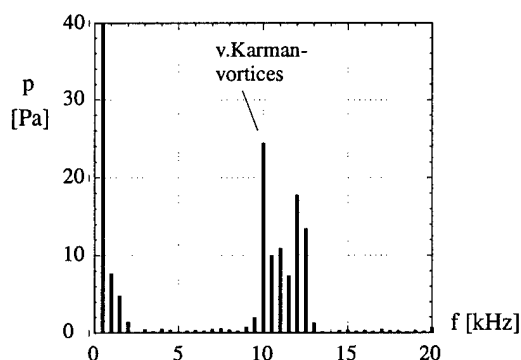

Figure 7. FFT-spectrum of unsteady pressure signal in the wake of the moving bar.
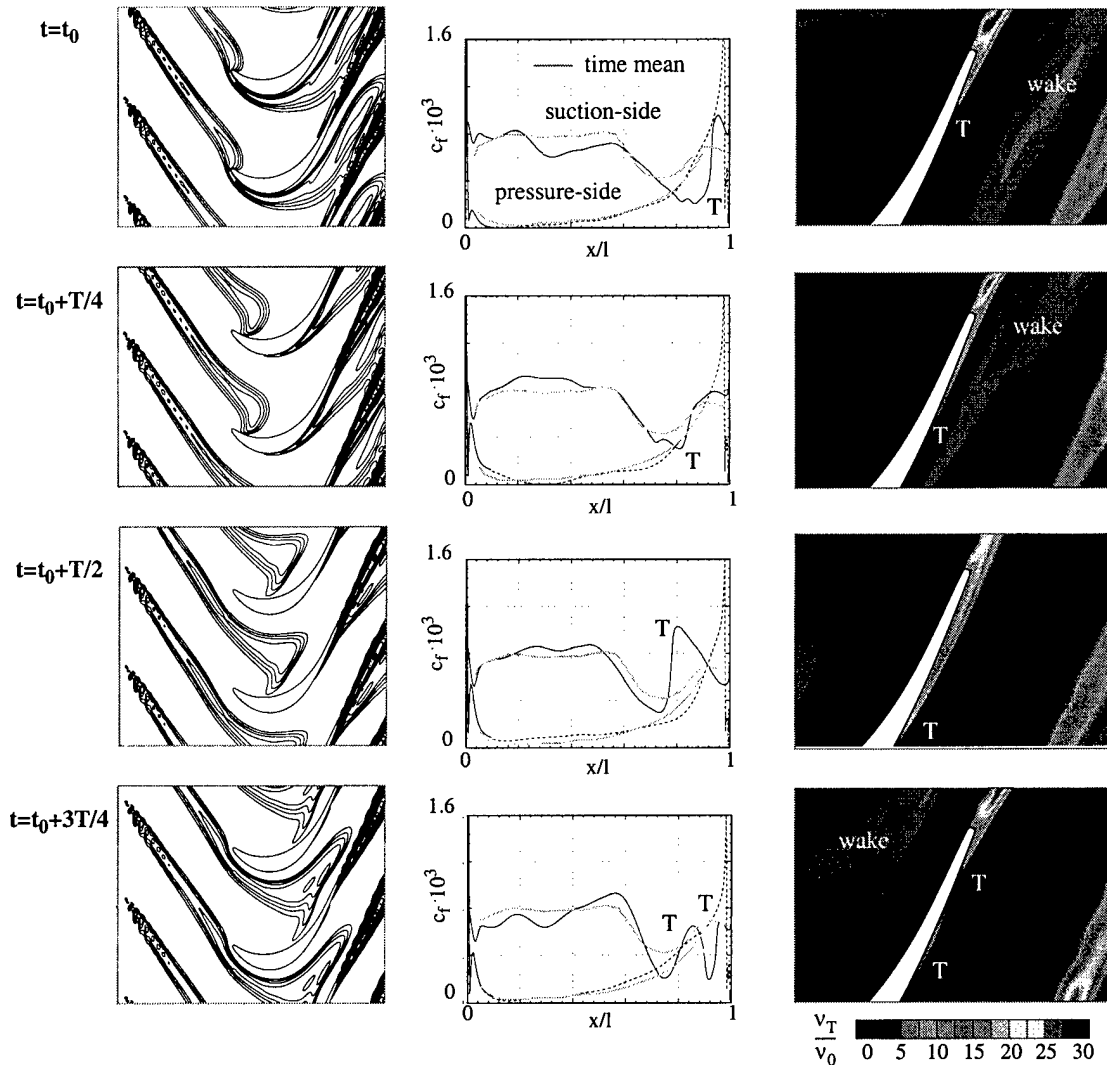
Figure 8. Temporal evolution of the wake disturbed unsteady flow. Sequence of eddy-viscosity isolines (left row), skin friction (center), contours of eddy-viscosity near trailing edge (right row).

To follow up on the temporal evolution of the flow, isolines of the instantaneous eddy-viscosity and skin friction have been supplied in figure 8 for 4 equispaced time-instants during a wake passing period. Once inside the blade passage, the wake is stretched and distorted due to the effect of the transverse pressure gradient across the passage. Close to the suction side the wake is substantially accelerated and near the pressure side it is decelerated.

To make the temporal variation more obvious, the time mean distribution of the skin friction has been added to the plots. In particular on the suction-side, the

interaction of the wake with the boundary-layer induces substantial fluctuations of the skin friction both in the laminar and the transitional part. Whereas in the laminar part the skin friction variation is rather of convective nature[20], it is in the transitional part mainly due to the production of Reynolds stresses. At the first time-instant shown ($t=t_0$), the wake has not yet reached the rearward part of the suction-side boundary-layer. Transition does then not start before x/L=0.92. Upon impingement of the wake ($t=t_0+T/4$), the transition zone starts to move upstream. At $t=t_0+T/2$, where the trailing edge of the wake has already proceeded beyond the trailing edge of
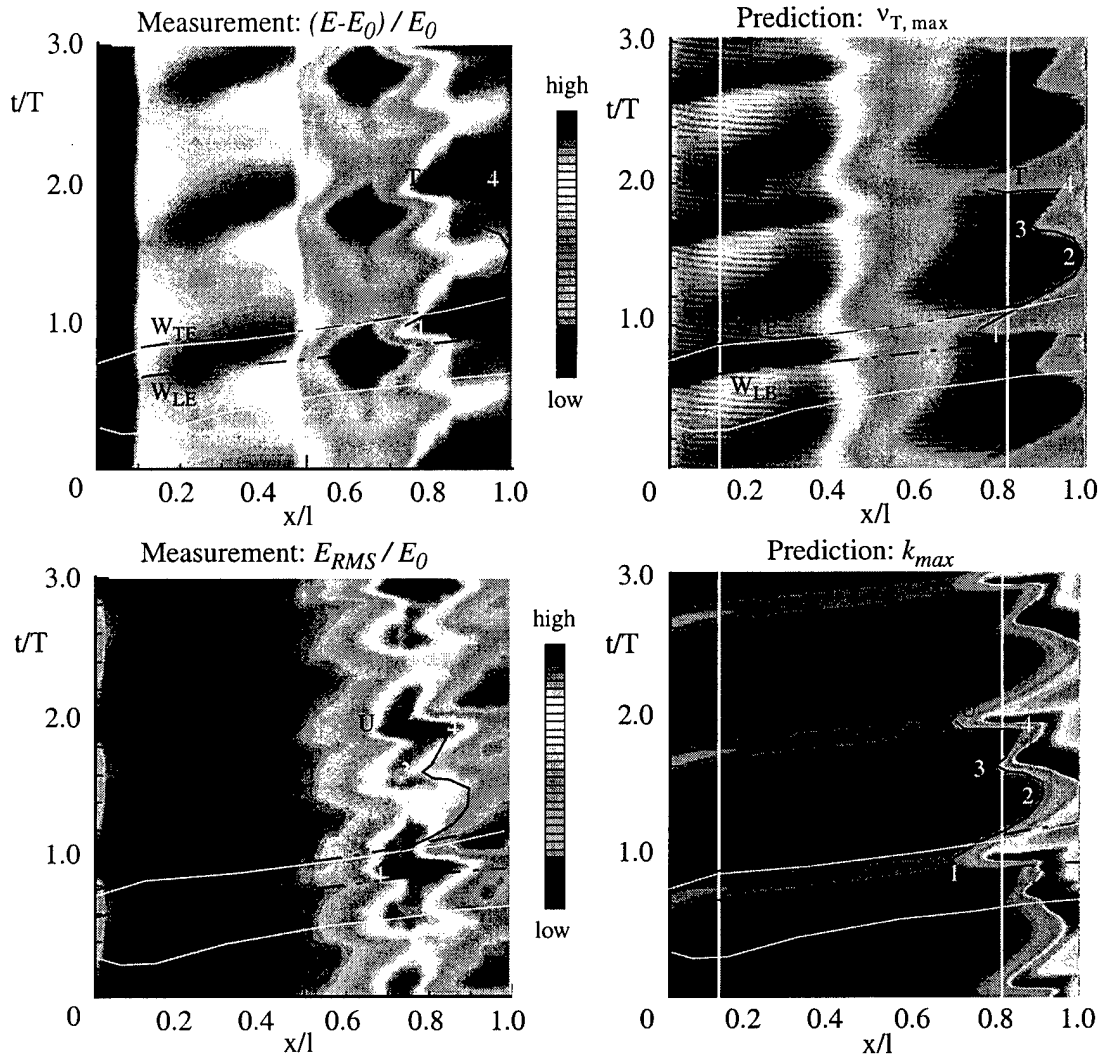
Figure 9. Temporal evolution of suction side boundary-layer parameters for 3 wake passing periods, measurements from Acton & Fottner[1,2] (left), computational results (right).

the blade, the transition start has reached its furthest upstream position (x/L=0.76). At the last time-instant shown (t=t_0+3T/4), the diminishing zone of elevated levels of eddy-viscosity suggests that the boundary-layer is in a process of becalming[15].

The wandering of the transition start location results in a fairly smooth increase of the time mean skin-friction (figure 8). It is interesting to note that the time mean is clearly different from the steady-state result shown in figure 4. While the steady-state skin friction shows a laminar separation-bubble of substantial extent, there is none in the time mean. This finding is in agreement with

the experimental observations[1,2]. Also, the skin friction in the laminar part of the suction-side boundary-layer is higher than in the corresponding steady-state distribution.

The disagreement of the steady-state and time-mean unsteady results observed here is in contrast to the transitional flow computations by Halstead et al.[16] who found "strong agreement" for the case of a compressor. Their computations were obtained using the unsteady boundary-layer code by Fan & Lakshminarayana[14].

American Institute of Aeronautics and Astronautics

Comparison with Hot Film Data

For a "semi-quantitative" comparison with the hot film measurement data by Acton & Fottner[1,2], space-time plots are considered. In figure 9, the abscissa show the wall shear or maximum kinetic energy of the suction-side boundary-layer and the ordinates are the time axes covering 3 wake passing periods. The comparison is semi-quantitative since the hot film data are in a raw form, i.e. in terms of the hot film anemometer output voltage $(E-E_0)/E_0$ normalized by the zero flow signal E_0. No calibration was performed by Acton & Fottner to obtain the shear stress using the proportionality $\sqrt[3]{\tau_w} \sim (E^2 - E_0^2)/E_0^2$. Nevertheless, a comparison of $(E-E_0)/E_0$ with the computed wall shear stress is meaningful since the *variation* of these quantities is of prime interest here. Also, the root mean square of the hot film signal E_{RMS}, which represents a measure for the turbulent fluctuations within the boundary-layer, are compared with the computed maximum kinetic energy k_{max} of the boundary-layer. As with the used one-equation turbulence model the kinetic energy is not readily available, the Bradshaw assumption $ak = \nu_T |\Omega|$ with $a=0.3$ is employed to obtain a rough estimate.

For better insight, the leading edge "W_{LE}" and trailing edge "W_{TE}" of the wake path, as can be clearly identified in the k_{max}-plot, have been copied into all space-time diagrams (dash-dotted black lines). Additionally, the wake paths as defined in the $\nu_{T, max}$-diagram of figure 10 have been drawn in white lines. The $\nu_{T, max}$ is the maximum eddy-viscosity of a given boundary-layer profile. As soon as the turbulent wake with its elevated values of eddy-viscosity reaches the freestream edge of the boundary-layer, $\nu_{T, max}$ starts to grow. However, not before the wake penetrates deeper into the boundary-layer to reach layers of increased vorticity will k_{max} grow. Therefore, in the k_{max}-plot the leading edge path of the wake lags the forward $\nu_{T, max}$-path. From figure 10 it can be observed that the k_{max} trace of the wake is accompanied by a decrease of the shape parameter H.

For an easier comparison, the temporal variation of the transition start location "T", as obtained in the calculation, has been marked (as solid black line) and copied into the measurement diagrams. To do so it was assumed that the transition start is always associated with a pronounced increase of the wall shear stress. It can be seen that the computed "T" variation provides a rather good match to the measurement. Note that both the measurement and the calculation produce two peaks (i.e. two extreme upstream positions) instead of a single one during a wake passing period!

The measured and computational space-time plots of the wall shear stress show that upon impingement of the wake the transition start "T" moves upstream. It reaches its furthest upstream position (at about x/L=0.75, location "1" in the figure 9) shortly before the trailing edge of the wake is reached. Then "T" is moving downstream almost up to the trailing edge, to location "2".The boundary-layer is becalming[15].
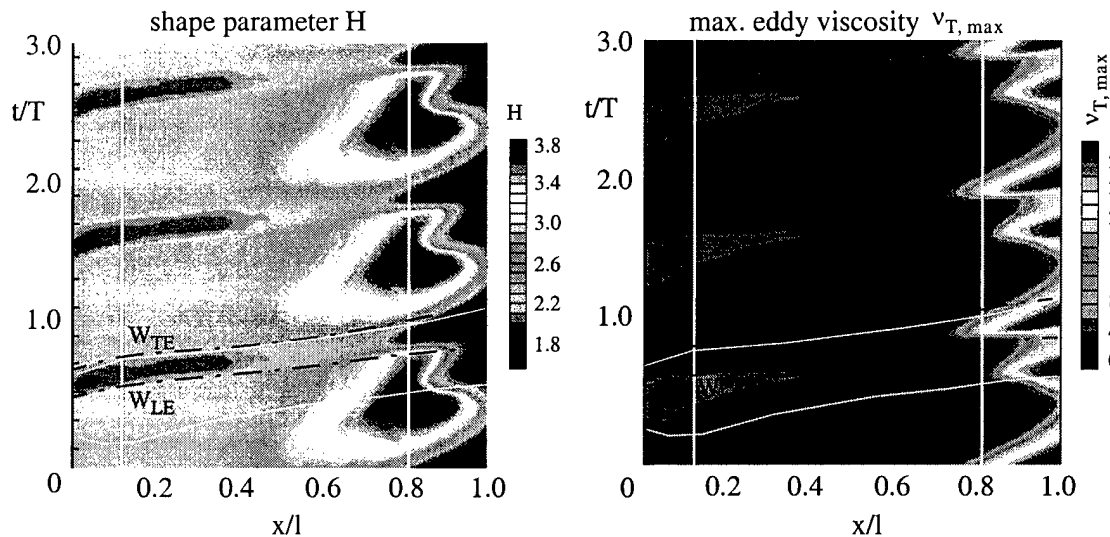

Figure 10. Temporal evolution of suction-side boundary-layer parameters for 3 wake passing periods, shape parameter (left), max. eddy-viscosity (right), computational results .

a) Test Case (Turbine Cascade)

b) Turbine (Cruise, Low Re)

A: laminar

B: transitional
C: turbulent   } wake-induced
D: becalmed

E: transitional
F: turbulent   } inbetween wakes
G: becalmed

W: wake path   I: path between wakes
L_B: transition start (wake-induced)
L_E: transition start (inbetween wakes)
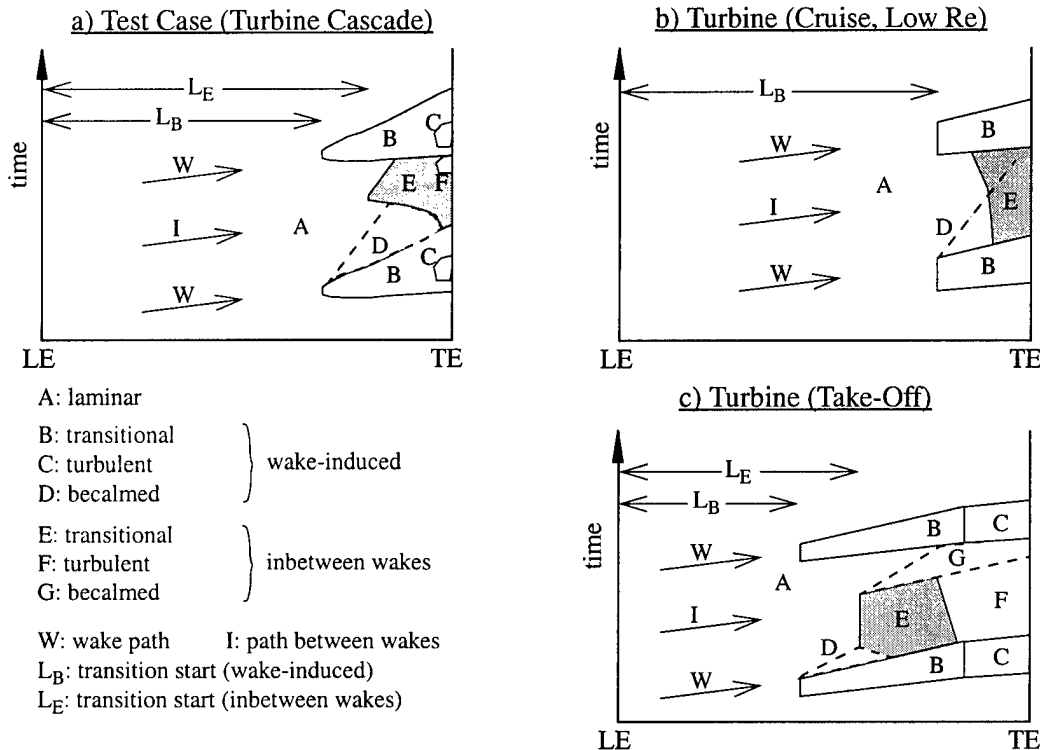
c) Turbine (Take-Off)

Figure 11. Composite pictures of boundary-layer development, (a) derived from the present computational results for a turbine cascade, (b) and (c) according to Halstead et al.[16].

Before the next wake enters the boundary-layer, "T" starts to propagate upstream to reach point "3". Then "T" slightly recedes to point "4" before a new cycle of wake-induced transition is introduced with the arrival of the next wake.

The space-time plots for the turbulent fluctuations (E_{RMS} and k_{Max} in figure 9) show a very similar temporal behavior. By comparison with the wall shear stress plots, it can be observed that the fluctuation level increases well before the skin friction does. The maximum of the *computed* fluctuation level, however, is reached further downstream than in the experiment. Moreover, the simulation is not capable to really reproduce the growth of the pretransitional disturbance level as is clearly evident in the E_{RMS}-plot. Primary instabilities (Tollmien-Schlichting waves) cannot be predicted with the current method. Although not all effects of the complicated wake-induced transition can be calculated with the current RANS approach, the agreement observed is quite remarkable and encouraging further assessment and refinement of the model.

The observed temporal evolution of the boundary-layer state is summarized in figure 11(a) in a fashion as

was done by Halstead et al.[16]. Due to the increased turbulence of the wake, transition reaches its most upstream extent, "B". The measurement as well as the computational results show that the wake-induced transition develops gradually. In the calculation this effect can be simulated because activating the production term of the turbulence model at a more upstream position results in a *gradual* increase of eddy-viscosity. The turbulent spots produced in "B" bring about a becalming process "D" where the transitional boundary-layer is gradually relaxing to a laminar one. Although a RANS analysis is fully blind of isolated turbulent spots, the *ensemble-averaged* effect of becalming can be simulated as gradual deactivation of the production term allows for a *gradual* decrease of the high eddy-viscosity levels generated earlier within the transitional strips. As a result the transitional boundary-layer asymptotically relaxes to a laminar one. Between the wake paths, a transitional zone "E" evolves. The calculation is capable of predicting it, since the diminishing Reynolds stresses of the becalming boundary-layer result in a less stable profile which the transition criterion is able to catch through an increasing shape parameter. It becomes clear

that important history effects of wake-induced transition can be effectively incorporated by manipulation of the production term, rather than by manipulation of the eddy-viscosity as is done in many algebraic intermittency models.

For comparison of the present observations of wake-induced transition in a turbine cascade, the composite pictures of boundary-layer development for a turbine at cruise 11(b) and take-off conditions 11(c) according to Halstead et al. are supplied.

Conclusion & Outlook

A time-accurate RANS method has been developed which is capable to effectively account for important effects of wake-induced transition in unsteady turbomachinery flow including the periodic upstream migration of the transition start, becalming as well as laminar separation-bubble induced transition.

The turbulence and transition model is based on the modification of the Spalart & Allmaras one-equation transport model and the use of a transition correlation by Drela. The model has been implemented into a parallel simulation system in such a way to allow for its application to unsteady multistage turbomachinery flow.

The validity of the approach has been demonstrated for the case of a turbine cascade subject to the unsteady wake of a moving bar. Although not all effects could be reproduced the agreement found is so good that the computation is believed to be a valuable supplement to experiments on wake-induced transition.

In future, the current approach will be applied to more validation cases. The refinement and assessment of the turbulence and transition model will continue. There are no plans to depart from the underlying concept of modifying the production term of the turbulence model.

Acknowledgments

References

1. Acton P., Fottner L., "Investigation of the Boundary-layer Development on a Highly Loaded Low Pressure Turbine Cascade under the Influence of Instationary Inlet Flow Conditions", Proceedings 8th ISUAAT, 1997.

2. Acton P., *Untersuchung des Grenzschichtumschlages an einem hochbekasteten Turbinengitter unter inhomogenen und instationären Zuströmbedingungen*, Dissertation, Universität BW München, 1998.

3. Bardina J.E., Huang P.G., Coakley T.J., "Turbulence Modeling Validation, Testing, and Development", *NASA Technical Memorandum*, TM 110446, 1997.

4. Drela M., 1995, "MISES Implementation of Modified Abu-Ghanam/Shaw Transition Criterion", MIT Aero-Astro.

5. Dorney D.J., Sharma O.P., "A Study of Turbine Performance Increases Through Airfoil Clocking", *AIAA-Paper*, 96-2816, 1996.

6. Dorney D.J., Gundy-Burlet, " Hot Streak Clocking Effects in a 1-1/2 Stage Turbine", AIAA Journal of Prop. and Power, Vol. 12., No. 3, pp. 619-620, 1996.

7. Engel, K., Eulitz,. F., Faden, M., and Pokorny, S., 1994, "Numerical Investigation of the Rotor-Stator Interaction in a Transonic Compressor Stage", AIAA-94-2834 .

8. Engel K., Eulitz F., Pokorny S., und Faden M., 1996, "3D Navier-Stokes Solver for the Simulation of the Unsteady Turbomachinery Flow on a Massively Parallel Hardware Architecture", *Notes on Numerical Fluid Dynamics*, Vieweg, Vol 52.

9. Eulitz F., Engel K., and Gebing, H., 1996, "Application of a one-equation eddy-viscosity model to unsteady turbomachinery flow", *Proc. of 3rd Int. Symp. on Eng. Turbulence Modelling and Measurements*, ed. H.W. Rodi, Elsevier Science.

10. Eulitz F., Engel K., Gebing H., "Numerical Investigation of the Clocking-Effects in a Multistage Turbine", ASME-Paper, 96-GT-26, Birmingham, 1996.

11. Eulitz F., Engel K., "Numerical Investigation of Wake-Interaction in a Low Pressure Turbine", ASME Paper 98-GT-563, 1998.

12. Eulitz F., Engel K., Nürnberger D., Schmitt S., Yamamoto K., 1998, "On Recent Advances of a Parallel Time-Accurate Navier-Stokes Solver for Unsteady Turbomachinery Flow", in *Computational Fluid Dynamics '98*, Proc. 4. ECCOMAS, Ed. Papailiou et al., Vol. 1, Part 1, pp. 252-258, John Wiley & Sons.

13. Eulitz F., *Numerische Simulation und Modellierung der instationären Strömung in Turbomaschinen*, dissertation to be submitted, Ruhr-Universität Bochum, 1999.

14. Fan S., Lakshminarayana B., 1996, "Computation and Simulation of Wake-Generated Unsteady Pressure and boundary-layers in Cascades: Part 1 and Part 2", *ASME J. of Turbomachinery*, Vol. 118, pp. 96-121.

15. Gostelow J.P., Walker G.J., Solomon W.J., Hong G., Melwani N., "Investigation of the Calmed Region Behind a Turbulent Spot", *ASME Journal of Turbomachinery*, Vol. 119, pp. 802-809, 1997.

16. Halstead D.E., Wisler D.C., Okiishi T.H., Walker G.J., Hodson H.P., Shin H.-W., 1997, "Boundary-Layer Development in Axial Compressors and Turbines: Part 1 of 4 - Composite Picture" and "Part 4 of 4 - Computations and Analyses", *ASME J. of Turbomachinery*, Vol. 119, pp. 114-127.

17. Hoeger M., *Theoretische und experimentelle Untersuchungen an Schaufelprofilen mit Grenzschichtumschlag über eine laminare Ablöseblase*, dissertation, Techn. Universität Braunschweig, ZLR-Forschungsbericht 92-01, 1992,

18. Mayle, R.E., 1991, "The Role of Laminar-Turbulent Transition in Gas Turbine Engines", *ASME J. of Turbomachinery*, Vol. 113, pp. 509-537.

19. Mayle R.E., Schulz A., "The Path to Predicting Bypass Transition", ASME-Paper, 96-GT-199, 1996.

20. Schmidt R.C., Patankar S.V., 1991, "Simulating boundary-layer Transition With Low-Reynoldsnumber k-e Turbulence Models: Part 1 - An Evaluation of Prediction Characteristic" and "Part 2 - An Approach to Improving the Predictions", *ASME J. of Turbomachinery*, Vol. 113, pp. 10-26.

21. Schulte V., Hodson H.P., "Unsteady Wake-Induced Boundary-Layer Transition in High Lift IP Turbines", ASME Paper, 96-GT-486, 1996.

22. Sharma, O.P., Ni, R.H., and Tanrikut, S., 1994, "Unsteady Flows in Turbines - Impact on Design Procedure", *AGARD Lecture Series 195*.

23. Sieger K., Schulz A., Crawford M.E., Wittig S., "An Evaluation of Low-Reynolds Number $k - \varepsilon$ Models for Predicting Transition under the Influence of Free-Stream Turbulence and Pressure Gradient", in *Engineering Turbulence Modelling and Experiments 2*, ed. W.Rodi & F. Martelli, pp. 593-602, Elsevier Science Publ. B.V., 1993.

24. Singer B., "Modeling the Transition Region", *Progress in Transition Modelling*, AGARD-Report 709, Kapitel 7, 1994.

25. Spalart, P., and Allmaras, S., 1992, " A One-Equation Turbulence Model for Aerodynamic Flows", AIAA-92-0439.

26. Steelant J., Dick E., "Calculation of Transition in Adverse Pressure Gradient Flow by Conditioned Equations", ASME-Paper, 96-GT-160, 1996.

27. Steelant J., Dick E., "A Transport Equation of a Turbulence Weighting Factor for Modelling By-Pass Transition", Proceedings der 4. ECCOMAS, Vol. 1, Part 1, pp. 535-540, John Wiley & Sons, 1998.

28. Volino J.R., "A New Model for Free-Stream Turbulence Effects on boundary-layers", ASME-Paper, 97-GT-122, 1997.

29. Walker G.J., Gostelow J.P., "Effects of Adverse Pressure Gradients on the Nature and Length of boundary-layer Transition", *ASME J. of Turbomachinery*, Vol. 112, pp. 196-205, 1990.

30. Walker G.J., "The Role of Laminar-Turbulent Transition in Gas Turbine Engines: A Discussion", *ASME Paper*, 92-GT-301, 1992.

31. Wilcox D.C., "Turbulence Modeling for CFD", DCW Industries, Inc., 1993.

Back